

SplitAMC: Split Learning for Robust Automatic Modulation Classification

Jihoon Park¹, Seungeun Oh¹, and Seong-Lyun Kim²

Department of Electrical and Electronic Engineering, Yonsei University, South Korea

¹{jhpark, seoh}@ramo.yonsei.ac.kr

²slkim@yonsei.ac.kr

arXiv:2304.12200v1 [eess.SP] 17 Apr 2023

Abstract—Automatic modulation classification (AMC) is a technology that identifies a modulation scheme without prior signal information and plays a vital role in various applications, including cognitive radio and link adaptation. With the development of deep learning (DL), DL-based AMC methods have emerged, while most of them focus on reducing computational complexity in a centralized structure. This centralized learning-based AMC (CentAMC) violates data privacy in the aspect of direct transmission of client-side raw data. Federated learning-based AMC (FedeAMC) can bypass this issue by exchanging model parameters, but causes large resultant latency and client-side computational load. Moreover, both CentAMC and FedeAMC are vulnerable to large-scale noise occurred in the wireless channel between the client and the server. To this end, we develop a novel AMC method based on a split learning (SL) framework, coined *SplitAMC*, that can achieve high accuracy even in poor channel conditions, while guaranteeing data privacy and low latency. In *SplitAMC*, each client can benefit from data privacy leakage by exchanging smashed data and its gradient instead of raw data, and has robustness to noise with the help of high scale of smashed data. Numerical evaluations validate that *SplitAMC* outperforms CentAMC and FedeAMC in terms of accuracy for all SNRs as well as latency.

Index Terms—Automatic modulation classification (AMC), split learning, federated learning, noise robustness, latency

I. INTRODUCTION

With the remarkable development of wireless communication, understanding the radio spectrum plays an essential role in various applications, such as cognitive radio and link adaptation [1], [2]. In this respect, automatic modulation classification (AMC) is emerging as a promising technology in a way that the receiver (Rx) identifies the modulation scheme of the corresponding transmitter (Tx) signal without prior information [3]. As the first of its kind, a traditional AMC method aims to achieve high detection probability through the likelihood function design [4]. However, due to its sensitivity to signal errors, it suffers from performance degradation and computational complexity, especially in the wireless environment where channel state information (CSI) is not given and channel gain fluctuates.

The feature-based AMC method can detour these problems by extracting hand-crafted features from the received signal and performing classification tasks. Going further, DL-based AMC can solve the computational complexity problem of likelihood-based AMC under a time-varying channel with deep learning (DL) framework [5]. The existing DL-based

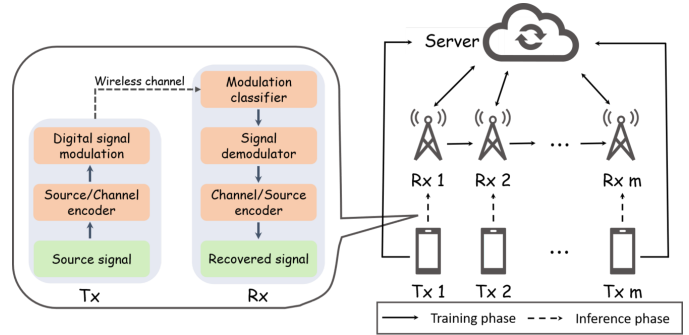


Fig. 1: An overview of communication system composed of Tx, Rx with AMC, and server.

AMC method is often rooted in a centralized architecture that enjoys dispersed data among multiple clients by direct local data aggregation on the server [6]. However, such centralized learning-based AMC (CentAMC) violates data privacy leakage while causing significant communication bottlenecks on the server-side. In order to guarantee data privacy, several AMC works apply a distributed learning framework to the AMC method. As its representative, FedeAMC [7], which combines federated learning (FL) with AMC, performs modulation classification by updating the local model through aggregation and redistribution of the model parameters between the server and clients. However, this model exchange incurs a huge communication overhead, so it is ill-suited for the large-sized model. *In addition, CentAMC and FedeAMC tend to be vulnerable to large-scale noise, leading to accuracy drop at low signal-to-noise ratio (SNR), highlighting the need for alternatives (see Table II).*

Towards a noise-robust, communication-efficient, and data-private AMC, this paper proposes a novel AMC method based on a split learning (SL) framework called *SplitAMC*. The *SplitAMC* divides the entire deep neural network (DNN) into two partitions depending on cut-layer, an upper model segment and a lower model segment, each stored by the server and clients, respectively. Under this model-split architecture, clients and the server communicate the cut-layer representations, so-called *smashed data*, and its corresponding gradients. In doing so, the *SplitAMC* can benefit from high accuracy over large-scale

noise, thanks to the scale of smashed data shown in Fig. 3. Also, exchanging smashed data instead of model parameters or raw data results in improved communication efficiency as well as data privacy guarantee of SplitAMC.

The contributions of this paper are summarized below:

- By revisiting the SL framework [8], we propose SplitAMC, an AMC method based on SL, that enables smashed data exchange instead of model parameters or raw data exchange.
- SplitAMC's smashed data exchange solves data privacy leakage that occurs in CentAMC, while reducing latency at the same time. Latency analysis for SplitAMC is available in Sec. IV.
- *Thanks to the large scale of the smashed data, SplitAMC has robust accuracy even in a large-noise environment, which is proven by experiments.*

The rest of the paper is organized as follows: Sec. II introduces a system model, including a single-carrier system-based signal model and a wireless channel model. Next, Sec. III describes the operation of our proposed SplitAMC in detail. In Sec. IV, the performance of SplitAMC is validated and analyzed through extensive simulations, compared to CentAMC as well as FedeAMC.

II. SYSTEM MODEL

In this section, we describe the network topology in which the DL-based approaches including the proposed SplitAMC run, and then sequentially describe the signal model and channel model of communication links included in the network.

A. Network Topology

As described in Fig. 1, we consider a communication system for AMC consisting of Tx-Rx pairs and server.

1) *Tx-Rx Communication Link*: Each Tx passes the source signal through the sampler and quantizer to perform analog-to-digital conversion (ADC) and encodes it, followed by selecting the modulation type, controlling the transmit power, and transmitting it to the corresponding Rx. Then, each Rx infers the modulation type of Tx through a modulation classifier and demodulates it based on it. Consequently, the goal of this paper is to train a modulation classifier with high accuracy, the key to the aforementioned communication system, via DL-based approach.

2) *Rx-Server Communication Link*: To achieve this goal, DL-based approaches perform additional communication between Rx and a server to train the model. At this time, an analog-modulated signal is assumed to be used. Although digital communication is widely used, it has notable drawbacks such as significant performance drop when deviating from target channel conditions (i.e., outage due to frequent channel fluctuations). On the other hand, analog communication can avoid this and even improve performance thanks to the regularizer effect of the noise [9]. Furthermore, analog-modulated signals can enjoy enhanced data privacy as well as latency gains by enabling over-the-air computation (AirComp) [10].

B. Communication Model

1) *Signal Model*: For Tx-Rx communication link, we use a regular signal model of the unknown single-input single-output single-carrier systems as in [11], [12]. Let $r(n)$ represent the unknown modulated signals at the Rx, denoted by:

$$r(n) = A_n e^{j(2\pi f_0 n T + \theta_n)} s(n) + \sigma(n), \quad (1)$$

$$n \in \{0, 1, \dots, N-1\},$$

where $s(n)$ and $\sigma(n)$ are the transmitted modulation signal and additive white Gaussian noise (AWGN), respectively. In addition, A_n is the signal amplitude of symbol n , following rayleigh channel fading, f_0 is the carrier frequency offset, θ_n is the time-varying carrier phase offset of symbol n , T is the symbol interval, and N is the number of symbols of the signals and also the number of samples to be used for training of the DL model.

The IQ sample, which is the training and test sample of DL, consists of in-phase (I) and quadrature (Q) parts of $r(t)$. Based on the received signal model, the IQ sample can be expressed as:

$$I = \{\text{Real}(r(0)), \text{Real}(r(1)), \dots, \text{Real}(r(N-1))\}, \quad (2)$$

$$Q = \{\text{Imag}(r(0)), \text{Imag}(r(1)), \dots, \text{Imag}(r(N-1))\},$$

where $\text{Real}(\cdot)$ and $\text{Imag}(\cdot)$ are functions for extracting values corresponding to the real and imaginary parts of the received signal $r(t)$.

Also, we can define the SNR of the received signal as follows:

$$\gamma_{data} = 10 \cdot \log_{10} \left(\frac{\sum_{n=0}^{N-1} |A_n s(n)|^2}{\sum_{n=0}^{N-1} |\sigma(n)|^2} \right) [dB]. \quad (3)$$

2) *Channel Model*: For Rx-server communication link, we consider the path-loss attenuation, channel fading, and noise, and its SNR is expressed by the following equation:

$$\gamma = 10 \cdot \log_{10} \left(\frac{h \cdot P \cdot d^{-\alpha}}{\sigma^2} \right) [dB], \quad (4)$$

where P is the transmit power, d is the distance between Tx and Rx, α is the path loss attenuation exponent, which usually corresponds to a value greater than or equal to 2, and σ^2 is the variance value of the AWGN in the wireless channel environment. Moreover, h indicates channel fluctuations and follows an exponential distribution with a mean of 1 ($h \sim \exp(1)$).

III. SPLIT LEARNING-BASED AMC

This section introduces the operation of SplitAMC method along with two existing AMC methods, CentAMC and FedeAMC. Let m be the subscript for Rx. Then, m -th Rx of set $\mathbb{M} = \{1, 2, \dots, M\}$ produces the IQ data samples via (2). For all $m \in \mathbb{M}$, the local dataset $D_m = (x_m, y_m)$ consists of IQ samples x_m and its corresponding ground-truth labels y_m . As depicted in Fig. 2c, to enable model-split architecture shown in [8], the entire model weight w_m is divided into the upper model segment w_s and the lower model segment $w_{c,m}$ based on the cut-layer.

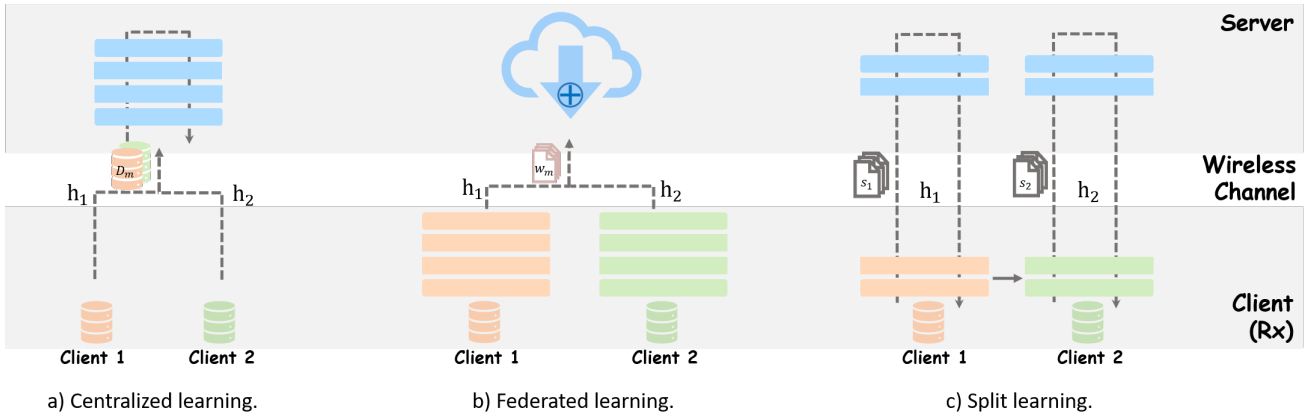


Fig. 2: Graphical illustrations of a) centralized learning, b) federated learning (FL), and c) split learning (SL).

A. Training Phase: The Operation of SplitAMC

Client-side Forward Propagation (FP). The m -th Rx randomly selects B data-label tuples from the local dataset D_m to compose a batch, and passes it through the lower model segment $w_{c,m}$ to generate smashed data s_m as follows:

$$s_m = f(x_m; w_{c,m}), \quad (5)$$

where $f(\cdot)$ denotes a function that maps x_m to s_m , determined by $w_{c,m}$. Then, the m -th Rx sends s_m to the server through an analog-modulated signal. \bar{s}_m reflecting the fluctuation and noise of the uplink (UL) wireless channel between Rx and the server in s_m is expressed as belows:

$$\bar{s}_m = h \cdot s_m + \mathbb{N} = h \cdot f(x; w_{c,m}) + \mathbb{N}, \quad (6)$$

where \mathbb{N} follows a zero-mean complex Gaussian distribution with variance σ^2 .

Server-side FP & Backpropagation (BP). To update the server-side model, the smashed data with Gaussian noise \bar{s}_m becomes the input of the upper model segment located on the server, yielding a *softmax output* \hat{y}_m as follows:

$$\hat{y}_m = g(\bar{s}_m; w_s), \quad (7)$$

where $g(\cdot)$ is a function that maps \bar{s}_m to \hat{y}_m due to the upper model segment w_s .

Then, by using the cross-entropy function, the loss L_{CE} can be calculated by:

$$L_{CE} = -\frac{1}{d_y} \sum_{i=1}^{d_y} y_{m,i} \log(\hat{y}_{m,i}), \quad (8)$$

where i is the subscript for element, so that $y_{m,i}$ and $\hat{y}_{m,i}$ are i -th elements of ground-truth label y_m and prediction \hat{y}_m , respectively, while d_y denotes the dimension of $y_{m,i}$.

With the aid of downlink (DL) communication in the cut-layer, BP is available allowing model update of Rx and server as follows:

$$\begin{bmatrix} w_{c,m} \\ w_s \end{bmatrix} \leftarrow \begin{bmatrix} w_{c,m} \\ w_s \end{bmatrix} - \eta \begin{bmatrix} \nabla_{w_{c,m}} L_{CE} \\ \nabla_{w_s} L_{CE} \end{bmatrix}, \quad (9)$$

where η and $\nabla_{w_{c,m}(w_s)}$ is the learning rate and the partial derivative with respect to $w_{c,m}(w_s)$, respectively.

After that, the m -th Rx transmits its lower model segment to the $(m+1)$ -th Rx as follows:

$$w_{c,m+1} \leftarrow w_{c,m}, \quad (10)$$

completing the single communication round of SplitAMC. The training operation of SplitAMC is detailed in the pseudocode of **Algorithm 1**.

B. Inference Phase: Performance Metrics

When the model $w_m = [w_{c,m}, w_s]$ converges after the K communication rounds, it enters the inference phase. To this end, two types of inference method can be considered. In the first case, all clients download the shared upper model segment of the server, then use it as a classifier for the modulated signal transmitted from the paired Tx, followed by demodulation. In other cases, we can consider an inference method in which the client and server communicate the smashed data of test data and prediction through UL and DL communication, respectively, while retaining the model. In both inference methods, it is possible to measure the performance of the test model w_m via the following performance metrics:

1) *Classification Performance:* The correct classification probability P_{cc} is employed to evaluate how accurately the test model w_m classifies the modulation scheme. When the total number of test samples is N_{test} , P_{cc} is defined by :

$$P_{cc} = \frac{N_{correct}}{N_{test}} \times 100[\%], \quad (11)$$

where $N_{correct}$ is the number of samples that successfully classified the modulation scheme among all N_{test} test samples.

2) *Latency Model:* Meanwhile, we can model the latency that occurs in the second inference method mentioned above or training phase. We divide the overall latency into communication latency T_{comm} , consisting of UL latency T_{UL} & DL latency T_{DL} , and computation latency T_{comp} . Here, we assume a static channel condition, i.e., $h = 1$ in (4) for convenience.

In terms of communication latency, it is proportional to the number of transmitted bits and inversely proportional to the

Algorithm 1: Model training method of SplitAMC framework.

1: **requirements:** $k = 0$, $w = [w_{c,m}, w_s]$, $D_m \forall m$
2: Hyperparameters:

- number of clients: $|\mathbb{M}| = M$,
- total number of communication rounds: K ,
- learning rate: η

3: **while** $k < K$ **do**
4: Client $m \in \mathbb{M}$:
5: **produces** s_m via (5) \triangleright *Client-side FP*
6: **unicasts** (s_m, y_m) to the server \triangleright *UL Communication*
7: Server:
8: **produces** \hat{y}_m via (7) \triangleright *Server-side FP*
9: **produces** L_{CE} via (8)
10: **updates** w_s via (9) \triangleright *Server-side BP*
11: **unicasts** $\nabla_{\bar{s}_m} L_{CE}$ \triangleright *DL Communication*
12: Client $m \in \mathbb{M}$:
13: **updates** $w_{c,m}$ via (9) \triangleright *Client-side BP*
14: **unicasts** $w_{c,m}$ to $(m + 1)$ -th Rx as in (10) \triangleright *Model Transfer*
15: $k \leftarrow k + 1$
16: **end while**

channel capacity, under the assumption of a static channel. Let L_a^b and β_a^b ($a \in \{SL, CL, FL\}$, $b \in \{UL, DL\}$) denote the number of parameters exchanged and the number of bits per parameter during b communication between Rx and server in a -based AMC method, respectively. Then, for the UL (DL) transmission rate $R_{UL(DL)} = BW \cdot \log_2(1 + \gamma)$ with γ in (4) where $h = 1$ and channel bandwidth BW , the latency for UL (DL) communication is $\frac{L_a^{UL(DL)} \cdot \beta_a^{UL(DL)}}{R_{UL(DL)}}$ for all a method.

Computational latency T_{comp} is classified into client-side latency (T_{client}) and server-side latency (T_{server}). Both latencies are expressed as the ratio of C to f , where C is the number of CPU cycles for processing FP as well as BP, and f is for client-side or server-side computational capacity (in CPU cycles/s). Assuming that the server-side computational capacity is infinite, T_{client} and T_{server} become unit computing time τ_{comp} and 0, respectively, during 1 communication round.

Table I summarizes T_{comm} and T_{comp} for 1 communication round of SplitAMC as well as FedeAMC and CentAMC. Note that the proposed SplitAMC can benefit in terms of computational latency, multiplied by the $\lambda \in [0, 1]$, depending on where the cut-layer is located.

C. Other AMC Methods

1) *CentAMC* [6]: As described in Fig. 2a, in CentAMC, all local datasets D_m are aggregated on the server through a wireless channel to form a single global dataset, becoming an input for a global model training of the server. By doing this, CentAMC easily obtains data diversity gain, but it causes a communication bottleneck when sending raw samples and violates data privacy guarantees.

2) *FedeAMC* [7]: In FedeAMC, the server distributes the global model to each local client $m \in \mathbb{M}$. Then, all

TABLE I: A summary of communication and computation latency for a single communication round of AMC methods.

Latency	T_{comm}		T_{comp}
	T_{UL}	T_{DL}	T_{client}
SplitAMC	$\frac{L_{SL}^{UL} \cdot \beta_{SL}^{UL}}{R_{UL}}$	$\frac{L_{SL}^{DL} \cdot \beta_{SL}^{DL}}{R_{DL}}$	$\lambda \cdot \tau_{comp}$
FedeAMC	$\frac{L_{FL}^{UL} \cdot \beta_{FL}^{UL}}{R_{UL}}$	$\frac{L_{FL}^{DL} \cdot \beta_{FL}^{DL}}{R_{DL}}$	τ_{comp}
CentAMC	$\frac{L_{CL}^{UL} \cdot \beta_{CL}^{UL}}{R_{UL}}$	$\frac{L_{CL}^{DL} \cdot \beta_{CL}^{DL}}{R_{DL}}$	-

local clients train the model using local dataset D_m . After that, as shown in Fig. 2b, local model parameters w_m are transmitted to the server through the wireless channel link. The server takes weighted averaging of aggregated local parameters, yielding a global model w , i.e., $w = (\sum_{m=1}^M |D_m| \cdot w_m) / \sum_{m=1}^M |D_m|$. This approach can take data diversity gain without direct data exchange, but large communication overhead occurs for large-sized models.

IV. EXPERIMENTAL RESULTS

This section evaluates SplitAMC's performance in terms of accuracy, convergence speed, and latency. For comparison, we use the aforementioned CentAMC and FedeAMC, and also SplitAMC with different cut-layer location. For the ResNet-18 model [13] with 4 residual blocks, SplitAMC_(1,3) and SplitAMC_(2,2) represent the SplitAMC framework when the cut-layers are located after the 1st and 2nd blocks, respectively.

For signal generation between Tx and Rx, Communications Toolbox in MATLAB is adopted. Considering the modulation schemes of QPSK, 16-QAM, and 64-QAM when SNR γ_{data} is 5, 10, and 15 dB, each modulation scheme includes 5000 data symbols, each composed of 1000 IQ samples. Prior to passing the CNN model, each IQ sample is transformed into a constellation image and resized to 64×64 dimensions as in [13], [14]. For experiment, we employ Intel i7-10700 CPU and GTX 3080Ti GPU, where the software environment is based on PyTorch v1.10.0 and CUDA v11.3 with Python v3.9.4. Other simulation parameters are given as: $M = 2$, batch size $B = 64$, total communication rounds $K = 50000$ steps, learning rate $\eta = 0.004$, transmit power $P = 100$ mW, distance between Rx-server $d = 100$ m, and path-loss exponent $\alpha = 2$.

A. Accuracy & Convergence Speed

Table II shows the classification accuracy of AMC methods according to different γ_{data} and channel environments. We consider two wireless communication environments depending on whether there is channel fluctuation, where the averaged SNR with channel fluctuation γ_{avg} and the fixed SNR without channel fluctuation γ_{fix} are the same as γ with $h = 1$ in (4). First, in all cases except for a few cases when γ_{data} is 10dB, the classification accuracy is high in the order of SplitAMC, CentAMC, and FedeAMC, showing the **noise-robustness** of

TABLE II: Classification performance P_{cc} of SplitAMC and comparison groups on datasets with different SNRs γ_{data} .

Channel SNR	$\gamma_{data} = 5\text{dB}$				10dB				15dB			
	Avg. SNR ($= \gamma_{avg}$)		Fixed SNR ($= \gamma_{fix}$)		Avg. SNR		Fixed SNR		Avg. SNR		Fixed SNR	
	-10dB	+10dB	-10dB	+10dB	-10dB	+10dB	-10dB	+10dB	-10dB	+10dB	-10dB	+10dB
SplitAMC _(1,3)	81.2 %	82.3 %	81.7 %	82.0 %	97.8 %	98.6 %	98.6 %	99.0 %	99.6 %	99.9 %	99.7 %	99.9 %
SplitAMC _(2,2)	81.1 %	81.1 %	80.8 %	82.5 %	97.7 %	98.9 %	98.6 %	99.0 %	99.6 %	99.9 %	99.8 %	99.9 %
CentAMC	66.6 %	67.5 %	68.4 %	68.7 %	77.3 %	78.4 %	77.9 %	78.7 %	97.4 %	97.5 %	97.7 %	97.8 %
FedeAMC	64.7 %	64.4 %	64.4 %	65.1 %	79.4 %	79.2 %	79.1 %	78.6 %	93.0 %	93.5 %	92.9 %	93.4 %

SplitAMC. This is rooted in the scale difference of parameters exchanged through the Rx-server link in SplitAMC and FedeAMC shown in Fig. 3, respectively. Considering also CentAMC, which uploads raw data with mean and variance normalized to 0.5, when noise of the same size is injected, the relatively large parameter scale of SplitAMC leads to small performance degradation. These parameter scale gaps can be compensated by increasing the transmit power (e.g., 200 times the transmit power [mW] for 200 times scale difference) which is unachievable given the client’s power constraints. Fig. 3 also implies a faster convergence speed of SplitAMC compared to FedeAMC through the parameter distribution change according to the number of steps, which is confirmed from the learning curve of Fig. 4.

Returning to Table II, the classification performance tends to deteriorate as γ_{data} or $\gamma_{avg}(\gamma_{fix})$ decreases and when channel fluctuations exist. γ_{data} and $\gamma_{avg}(\gamma_{fix})$ are respectively related to the noise inherent in the IQ data itself and the noise applied to the resized constellation image, and it is confirmed that the performance reduction for γ_{data} is noticeable among them, indicating the importance of the Tx-Rx communication link state. The existence of channel fluctuations reduces the accuracy since it is difficult to learn a generalized model in the training phase. Focusing on the gap in classification accuracy between AMC methods, the worse the communication channel conditions, the greater the difference, proving the effectiveness of SplitAMC. In addition, in Table II as well as in Fig. 4, there is no significant difference in performance in terms of accuracy or convergence speed for cut-layer in SplitAMC.

B. Latency Measurement for Training

Fig. 5 compares latency between AMC methods according to the ratio of τ_{comp} and τ_{comm} , which is the reciprocal of up-link rate R_{UL} . Here, to reflect the UL-DL asymmetric capacity of the cellular network, it is assumed that $R_{DL} = 10R_{UL}$. Other parameters for calculating latency are as follows: $\beta_a^b = 32$ bits for all a & b , $\gamma = 10$ dB for UL communication, $BW = 10$ MHz, and 50 total communication rounds.

The first thing to note is that overall latency performance improves when the ratio is 10:1, i.e., when τ_{comm} is small. In other words, this means that the communication payload size of UL, which determines UL latency, is the main factor influencing latency. Thanks to the low dimension of smashed

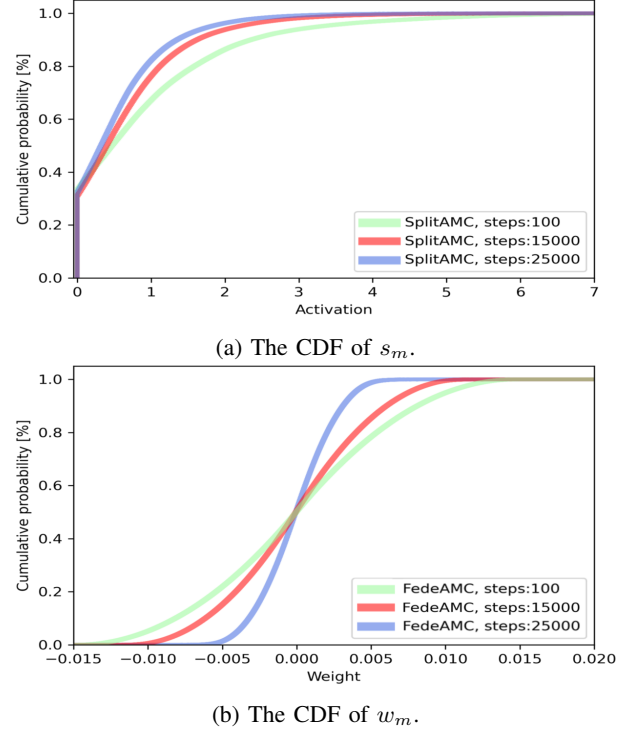


Fig. 3: Cumulative distributions of parameter values in SplitAMC and FedeAMC for different steps.

data, SplitAMC outperforms the baselines, except for CentAMC at 10:1. In the case of CentAMC, T_{comp} converges to 0 under our premise that the server-side computational capacity is infinite, and this dramatically reduces overall latency when $\tau_{comp} : \tau_{comm}$ is 10:1. Regarding the cut-layer, the closer the cut-layer is to the input layer, the better in terms of latency. This is because the client-side computational latency varies according to λ as the cut-layer location changes, although there is no huge gap in the dimension of activation. When considering its accuracy and convergence speed together, it is optimal to place the cut-layer close to the input layer in SplitAMC, even beneficial in terms of client memory. Note that the above method is also applicable for the inference phase, by replacing the payload size.

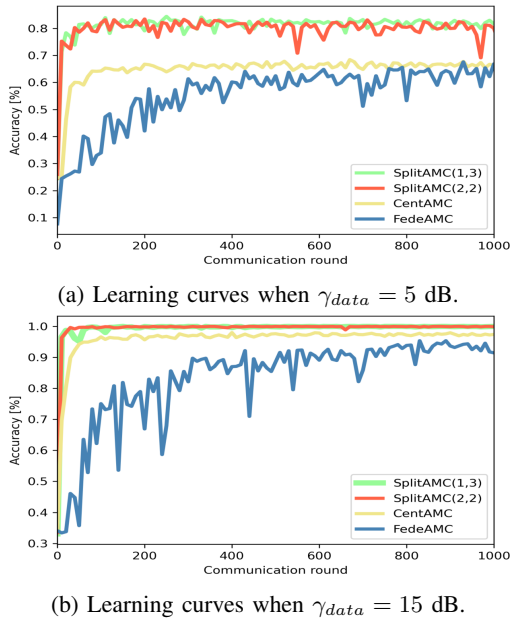


Fig. 4: Learning curves of AMC methods w.r.t different γ_{data} .

V. CONCLUSION

In this paper, we revisited the SL framework and applied it to AMC to design SplitAMC framework. Unlike the existing AMC methods, in SplitAMC, the client and server each hold a fraction of the entire model and exchange the output and gradient of the cut-layer, thereby resulting in a small memory size, computational cost, and communication payload size. Moreover, with the help of large scale inherent in smashed data, SplitAMC guarantees noise-robustness that can achieve high accuracy even when noise with large variance is ejected. Numerical evaluations validate the accuracy, convergence speed, and latency of SplitAMC. It is worth noting that this work focused on connecting parametric properties in distributed learning (i.e., scale and dimension) to metrics in wireless communication (i.e., classification accuracy and latency). As a future work, we will exploit the classification performance as the number of clients increases as in [15]. Also, investigating the accuracy-privacy tradeoff for noise variance [16] in SplitAMC could be an interesting topic, deferred as future work.

ACKNOWLEDGEMENT

This work was supported by Institute of Information & communications Technology Planning & Evaluation(IITP) grant funded by the Korea government(MSIT) (No.2022-0-00420,Development of Core Technologies enabling 6G End-to-End On-Time Networking & No.2021-0-00270, Development of 5G MEC framework to improve food factory productivity, automate and optimize flexible packaging)

REFERENCES

[1] L. Liu, Y. Zhou, W. Zhuang, J. Yuan, and L. Tian, "Tractable coverage analysis for hexagonal macrocell-based heterogeneous udns with

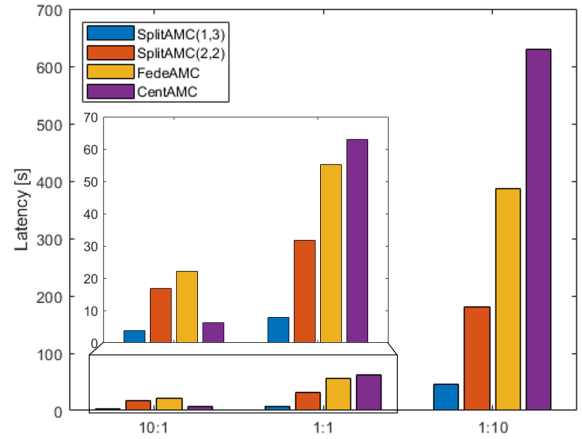


Fig. 5: Latency according to the ratio of τ_{comp} to τ_{comm} .

- adaptive interference-aware comp," *IEEE transactions on wireless communications*, vol. 18, no. 1, pp. 503–517, 2018.
- [2] S. Luan, Y. Gao, T. Liu, J. Li, and Z. Zhang, "Automatic modulation classification: Cauchy-score-function-based cyclic correlation spectrum and fc-mlp under mixed noise and fading channels," *Digital Signal Processing*, vol. 126, p. 103476, 2022.
- [3] L. Liu, Y. Zhou, J. Yuan, W. Zhuang, and Y. Wang, "Economically optimal ms association for multimedia content delivery in cache-enabled heterogeneous cloud radio access networks," *IEEE Journal on Selected Areas in Communications*, vol. 37, no. 7, pp. 1584–1593, 2019.
- [4] F. Hameed, O. A. Dobre, and D. C. Popescu, "On the likelihood-based approach to modulation classification," *IEEE transactions on wireless communications*, vol. 8, no. 12, pp. 5884–5892, 2009.
- [5] T. Huynh-The *et al.*, "Automatic modulation classification: A deep architecture survey," *IEEE Access*, vol. 9, pp. 142950–142971, 2021.
- [6] Y. Wang, J. Yang, M. Liu, and G. Gui, "Lightamc: Lightweight automatic modulation classification via deep learning and compressive sensing," *IEEE Transactions on Vehicular Technology*, vol. 69, no. 3, pp. 3491–3495, 2020.
- [7] Y. Wang *et al.*, "Federated learning for automatic modulation classification under class imbalance and varying noise condition," *IEEE Transactions on Cognitive Communications and Networking*, vol. 8, no. 1, pp. 86–96, 2021.
- [8] O. Gupta and R. Raskar, "Secure training of multi-party deep neural network," Aug. 25 2020. US Patent 10,755,172.
- [9] X. Zhou *et al.*, "Learning with noisy labels via sparse regularization," in *Proceedings of the IEEE/CVF International Conference on Computer Vision*, pp. 72–81, 2021.
- [10] Y. Koda, J. Park, M. Bennis, P. Vepakomma, and R. Raskar, "Airmixml: Over-the-air data mixup for inherently privacy-preserving edge machine learning," in *2021 IEEE Global Communications Conference (GLOBECOM)*, pp. 01–06, IEEE, 2021.
- [11] B. Dong *et al.*, "A lightweight decentralized learning-based automatic modulation classification method for resource-constrained edge devices," *IEEE Internet of Things Journal*, 2022.
- [12] S. Zheng, P. Qi, S. Chen, and X. Yang, "Fusion methods for cnn-based automatic modulation classification," *IEEE Access*, vol. 7, 2019.
- [13] Y. Lin, Y. Tu, Z. Dou, and Z. Wu, "The application of deep learning in communication signal modulation recognition," in *IEEE/CIC International Conference on Communications in China (ICCC)*, pp. 1–5, 2017.
- [14] S. Peng *et al.*, "Modulation classification based on signal constellation diagrams and deep learning," *IEEE transactions on neural networks and learning systems*, vol. 30, no. 3, pp. 718–727, 2018.
- [15] S. Oh *et al.*, "Locfedmix-sl: Localize, federate, and mix for improved scalability, convergence, and latency in split learning," in *Proceedings of the ACM Web Conference 2022*, pp. 3347–3357, 2022.
- [16] S. Oh *et al.*, "Differentially private cutmix for split learning with vision transformer," in *First Workshop on Interpolation Regularizers and Beyond at NeurIPS 2022*, 2022.